

CrystEngComm

Accepted Manuscript



This is an *Accepted Manuscript*, which has been through the Royal Society of Chemistry peer review process and has been accepted for publication.

Accepted Manuscripts are published online shortly after acceptance, before technical editing, formatting and proof reading. Using this free service, authors can make their results available to the community, in citable form, before we publish the edited article. We will replace this *Accepted Manuscript* with the edited and formatted *Advance Article* as soon as it is available.

You can find more information about *Accepted Manuscripts* in the [Information for Authors](#).

Please note that technical editing may introduce minor changes to the text and/or graphics, which may alter content. The journal's standard [Terms & Conditions](#) and the [Ethical guidelines](#) still apply. In no event shall the Royal Society of Chemistry be held responsible for any errors or omissions in this *Accepted Manuscript* or any consequences arising from the use of any information it contains.

Recent advances on porous homochiral coordination polymers containing amino acid synthons

Xiu-Li Yang,^{ab} and Chuan-De Wu*^a

^a*Center for Chemistry of High-Performance and Novel Materials, Department of Chemistry, Zhejiang University, Hangzhou, 310027, P. R. China*

^b*Key Laboratory for Advanced Technology in Environmental Protection of Jiangsu Province, Yancheng Institute of Technology, Yancheng, 224051, P. R. China*

E-mail: cdwu@zju.edu.cn

Abstract

Natural amino acids are the basic building units and functional groups in biological organisms. Attracted by the unique properties derived from amino acids and their derivatives, such as chiral recognition and selective binding to substrate molecules, they have been used as building blocks for the construction of a variety of homochiral metal-organic coordination polymers (MOCPs). Given the fact that most of the natural amino acids do not have sufficient coordination donors and rigid backbones for the construction of higher porous MOCPs, several effective strategies have been therefore established to improve the porosity and rigidity of coordination networks containing amino acid residues. Those homochiral MOCPs exhibit intriguing structural patterns and interesting properties, which have been realized applications in a number of fields of asymmetric catalysis, luminescence, adsorption, separation, magnetics, second-order nonlinear optics (NLO) and conduction. This highlight is aimed to give an account of recent advances on the synthesis and applications of homochiral MOCPs that contain amino acid synthons.

1. Introduction

In the past two decades, metal-organic coordination polymers (MOCPs) or metal-organic frameworks (MOFs), constructed from organic building blocks connected with metal ions/metal clusters, have been made great progress in terms of structural chemistry, and applications in diverse fields of gas storage and separation,

heterogeneous catalysis, luminescence, sensing, magnetics, second-order nonlinear optics (NLO), thin film, biomedical imaging and drug delivery.¹⁻⁹ Since chirality is an essential element in many biological processes, great endeavor has been focused on the development of homochiral MOCPs for chirality-related applications, such as asymmetric catalysis, chiral separation and enantioselective sensing.¹⁰⁻¹² Over the past decade, several effective strategies have been established on the design and synthesis of homochiral MOCPs. The most straightforward and efficient pathway is to derive chiral ligands from chiral organic moieties, such as BINOL derivatives,¹³ metal-Salen series¹⁴ and natural amino acid derivatives.¹⁵⁻¹⁸ To improve the porosity of homochiral MOCPs, the secondary rigid ligands are frequently introduced as auxiliary pillars.¹⁹⁻²¹ Additionally, post-modification of achiral porous coordination frameworks with chiral moieties is also an efficient pathway.^{22,23}

Due to their special biological activities, species diversity, selective substrate-binding function and flexible coordination ability, natural amino acids and their derivatives have been attractive synthons for the construction of homochiral MOCPs. However, their limited coordination sites and preferred chelating coordination modes to metal ions often make it very difficult to synthesize higher dimensional porous MOCPs. Therefore, several strategies have been developed to improve the bridging ability of amino acids for the intention to synthesize higher porous MOCPs. Since the carboxylic acid and amino groups of amino acids are chemically active, they can be selectively modified with different organic moieties. The carboxylic acid groups can react with amino groups to form amides or peptides. The amino groups are more active, which can be modified through multiple reactions, such as acylation, condensation with aldehydes and C-N cross coupling with organic halogens, to expand amino acids into multidentate connectors. Moreover, introduction of the secondary rigid bridging ligands can also efficiently improve the porosity of homochiral MOCPs. Additionally, dangling amino acid residues on the backbones of highly porous achiral MOCPs either on the metal ions or rigid organic ligands by in situ or post-synthesis is frequently used to realize the chirality-related applications. The applications of amino acids based MOCPs include asymmetric catalysis,²⁴⁻²⁵

luminescence,²⁶⁻²⁸ adsorption,^{29,30} separation,³¹ magnetics,³² second-order nonlinear optics (NLO)³³ and conduction.³⁴

2. Homochiral MOCPs built from single amino acids

The Jacobson group reported an interesting strategy for the construction of 3D porous homochiral MOCPs upon tuning the pH values of reaction solutions according to the dependence between the structures of MOCPs and acid-base conditions.²⁹ At pH = 5.0 tuned by Et₃N, the mixture of L-Asp and NiCl₂ results a 1D MOCP [Ni₂O(L-Asp)(H₂O)₂] \cdot 4H₂O.³⁵ Upon increasing the pH value to 6.1, a mixture of [Ni₂O(L-Asp)(H₂O)₂] \cdot 4H₂O and [Ni_{2.5}(OH)(L-Asp)₂] \cdot 6.55H₂O (ca. 2:1) was obtained. It will synchronously form both [Ni_{2.5}(OH)(L-Asp)₂] \cdot 6.55H₂O and Ni(OH)₂ when the pH value is increased to 7.2. Moreover, [Ni₂O(L-Asp)(H₂O)₂] \cdot 4H₂O can be further transferred to [Ni_{2.5}(OH)(L-Asp)₂] \cdot 6.55H₂O induced by Et₃N, because the structure of [Ni_{2.5}(OH)(L-Asp)₂] contains 1D helical chains [Ni₂(OH)(L-Asp)] linked through [NiAsp₂]²⁻ bridges (Fig. 1). In the 3D porous structure of [Ni_{2.5}(OH)(L-Asp)₂], the helical chains of edge- and corner-shared Ni octahedra are connected through Ni-O-Ni linkers, resulting in 1D helical channels of $\sim 5 \times 8 \text{ \AA}^2$ in dimensions. [Ni_{2.5}(OH)(L-Asp)₂] represents a rare example of 3D porous homochiral MOCPs based on single amino acids, which exhibits significant uptakes of N₂ and 1,3-butanediol molecules, and interesting ferrimagnetic behavior below 5.5 K.

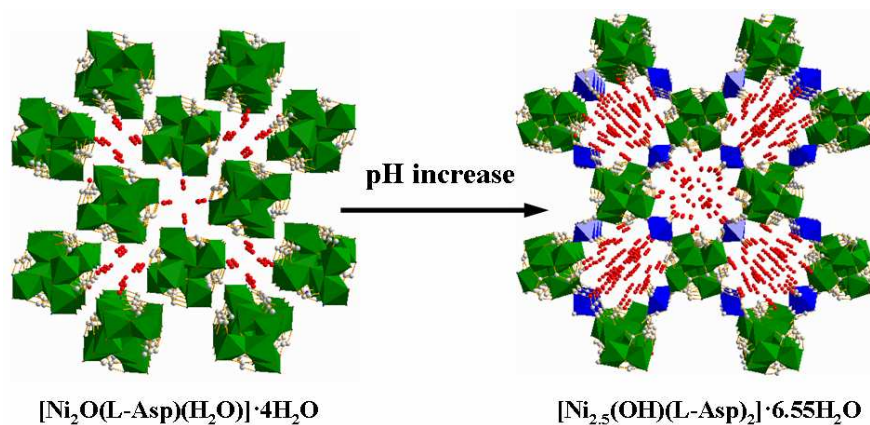


Fig. 1. Illustration of the transformation of nickel L-aspartates from 1D [Ni₂O(L-Asp)(H₂O)₂] \cdot 4H₂O to 3D porous [Ni_{2.5}(OH)(L-Asp)₂] \cdot 6.55H₂O structures induced by Et₃N. CCDC nos. 235205 and 622439.

3. Homochiral MOCPs built from amino acids and secondary rigid ligands

The pore structures of homochiral MOCPs play important roles on exertion of the functions of amino acids by directing molecular recognition. However, there are many difficulties in the construction of highly porous materials with single amino acids, due to their flexible backbones and limited coordination donors. Therefore, secondary rigid ligands are necessarily introduced to compensate the shortcoming of amino acids. For example, 4,4'-bipyridine (4,4'-bpy) is a rigid, bidentate and neutral organic ligand, which can provide significant help on the construction of porous homochiral MOCPs by connecting with adjacent amino acid-metal secondary building units (SBUs).

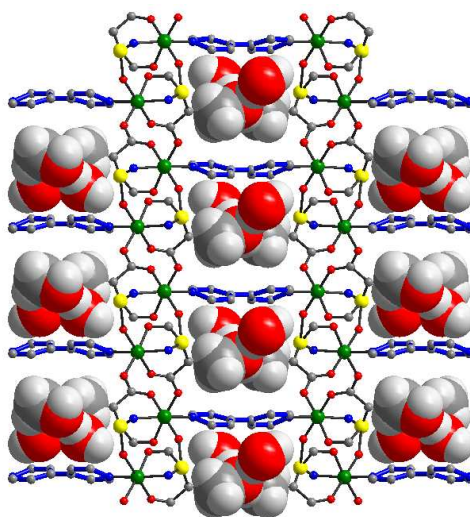


Fig. 2. A view of the 3D porous structure of $[\text{Ni}_2(\text{L-Asp})(\text{bpy})]$, built from $\text{Ni}(\text{L-Asp})$ layers connected by 4,4'-bpy (the guest molecules are represented in space-filling model). CCDC no. 607296.

Rosseinsky and coworkers reported a 3D porous homochiral MOCP $[\text{Ni}_2(\text{L-Asp})(\text{bpy})] \cdot 1.28\text{CH}_3\text{OH} \cdot 0.72\text{H}_2\text{O}$ that is built from $\text{Ni}(\text{L-Asp})$ linked by 4,4'-bpy.³¹ In the crystal structure, $\text{Ni}(\text{L-Asp})$ layers are connected with 4,4'-bpy to form narrow channels of $3.8 \times 4.7 \text{ \AA}^2$ in dimensions (Fig. 2). The desolvated sample of $[\text{Ni}_2(\text{L-Asp})(\text{bpy})]$ can retain the original pore structure for chiral separation. It is interesting that the enantioselectivity is highly dependent on the size of different diols as confirmed by the semi-empirical quantum-mechanical calculations at the PM3

level, in which the highest ee value of 53.77% is achieved for the bulky 2-methyl-2,4-pentanediol.

Polyoxometalates (POMs) are a class of functional metal-oxygen anionic clusters, which have high charge density and abundant oxygen donors on their surfaces. Hence, POMs can combine with different metal ions through strong electrostatic interactions and coordination bindings. Wang *et al.* reported a pair of 3D porous homochiral hybrid enantiomorphs $\text{KH}_2[(\text{D}-\text{C}_5\text{H}_8\text{NO}_2)_4(\text{H}_2\text{O})\text{Cu}_3][\text{BW}_{12}\text{O}_{40}] \cdot 5\text{H}_2\text{O}$ and $\text{KH}_2[(\text{L}-\text{C}_5\text{H}_8\text{NO}_2)_4(\text{H}_2\text{O})\text{Cu}_3][\text{BW}_{12}\text{O}_{40}] \cdot 5\text{H}_2\text{O}$ assembled from $[\text{BW}_{12}\text{O}_{40}]^{5-}$ and L- or D-proline.¹⁶ In the crystal structures, the Keggin unit $[\text{BW}_{12}\text{O}_{40}]^{5-}$ acts as a bidentate ligand to connect with two polymer chains of copper-proline, resulting unique 3D porous frameworks with 1D opening channels of $10.6 \times 7.2 \text{ \AA}^2$ in dimensions (Fig. 3). CD spectra indicate that the chirality was effectively transferred from L- or D-proline to the whole frameworks.

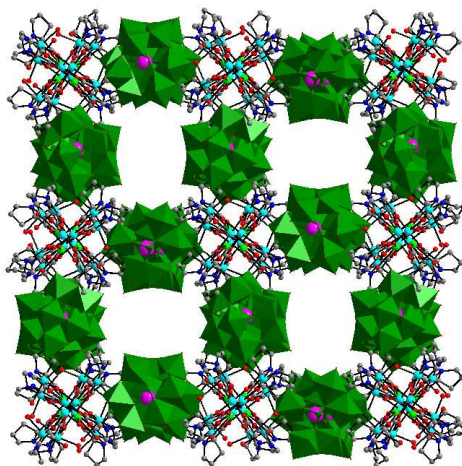


Fig. 3. A view of the 3D open framework of $\text{KH}_2[(\text{D}-\text{C}_5\text{H}_8\text{NO}_2)_4(\text{H}_2\text{O})\text{Cu}_3][\text{BW}_{12}\text{O}_{40}]$ along the *c* axis, in which the 1D opening channels are formed from POM anions linking to copper-proline chains. CCDC no. 285623.

4. Homochiral MOCPs built from peptides

Peptides, the condensation products of amino acids, have multiple chiral centers and rich coordination sites of carboxylic acid, amino and amide groups along with flexible backbones, which can improve the structural multiplicity of homochiral MOCPs. The

first example of peptide-based MOCPs was reported by Manton and coworkers.³⁶ An oligo-peptide *Z*-L-Val-L-Glu(OH)OH was employed to prepare two complexes, MPF-2 ($C_{23}H_{39}CaN_3O_{12}$) and MPF-9 ($C_{23}H_{44}CuN_5O_{10}$), in which the structure of MPF-9, based on the results of powder X-ray diffraction analysis, is a supramolecular network linked by hydrogen bondings.

Rosseinsky and coworkers reported an interesting solvent-adaptable porous material $[Zn](Gly-Ala)_2$ ·solvent based on dipeptide Gly-Ala and Zn^{II} ions.¹⁷ In the crystal structure, each dipeptide coordinates with two zinc ions while each zinc ion coordinates to four dipeptides to form a 2D grid network, containing 1D hourglass-shaped channels (Fig. 4). The solvent molecules can be reversibly removed and restored in the 1D channels, which presents dynamic properties. It is interesting that the desolvated sample will close the pores, which can be gradually and cooperatively opened that are triggered by small polar molecules.

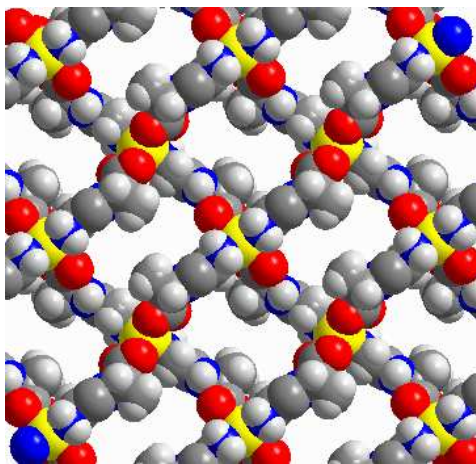


Fig. 4. The 2D grid network of $[Zn(Gly-Ala)_2]$ with 1D hourglass-shaped channels as viewed along the *c* axis. CCDC no. 764870.

Besides of the flexibility, the rigidity can also be achieved in peptide-based MOCPs as demonstrated from recent work of the same group.³⁷ The authors used Gly-Thr dipeptide to build a homochiral MOCP $[Zn(Gly-Thr)_2] \cdot CH_3OH$. In $Zn(Gly-Thr)_2$, each dipeptide connects with two zinc ions to propagate into 2D grid-like layers, which are further packed together in an ...AA... stacking pattern,

generating 1D channels that are occupied by methanol molecules (Fig. 5). The desolvated $\text{Zn}(\text{Gly-Thr})_2$ is robust and crystalline because there is strong hydrogen bonding interaction between N-terminus amino groups and OH groups of the threonine side chain. Driven by the intra-layer hydrogen bonding interaction, $\text{Zn}(\text{Gly-Thr})_2$ behaves as a rigid porous material to selectively adsorb CO_2 over CH_4 with a single-component separation ratio of 14:1 (wt%) at 1 bar and 273 K.

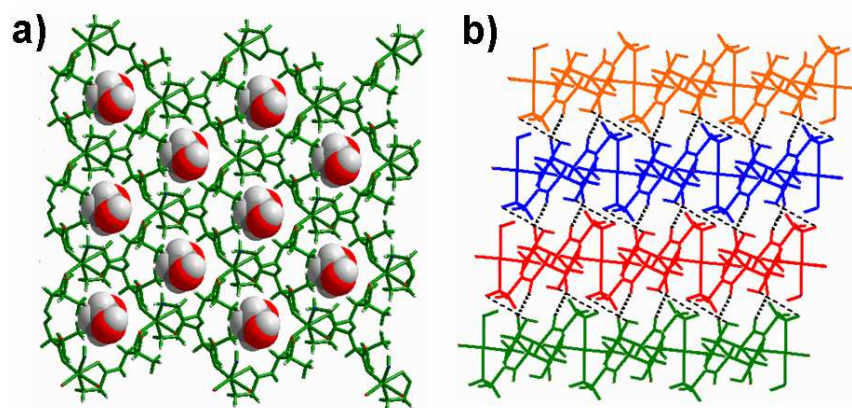


Fig. 5. (a) A view of the 2D grid-like layer structure of $[\text{Zn}(\text{Gly-Thr})_2]\cdot\text{CH}_3\text{OH}$ containing methanol molecules; and b) the adjacent layers linked by strong hydrogen-bonding interaction. CCDC no. 874399.

5. Homochiral MOCPs built from amino acid derivatives

To improve the bridging ability of amino acids, several effective strategies have been established by introducing more coordination donors, such as to react the amino groups with aldehydes,^{15,24,27,33,34,38-40} with organic halides *via* C-N coupling reaction,^{26,41} and with acyl chlorides.⁴²⁻⁴⁵ Cyclization of amino acids is also able to improve the rigidity and bridging ability of amino acids.³⁰ Additionally, to attach amino acid residues on the backbones of rigid ligands is frequently used to develop highly porous homochiral coordination frameworks from their achiral analogues.^{9,21,25,46}

5.1 Homochiral MOCPs built from reduced Schiff bases

The reduced Schiff bases of amino acid derivatives contain multiple N and O

coordination donors and flexible structural backbones, which have been used to produce a variety of homochiral MOCPs with intriguing topological patterns and interesting properties. Vittal and coworkers synthesized a reduced Schiff base H₃sglu from salicylaldehyde and L-glutamic acid, which was reacted with nickel nitrate to afford a helical MOCP [(H₂O)₂⊂{Ni(Hsglu)(H₂O)₂}]·H₂O.¹⁵ In the structure, Ni^{II} ion is chelated and bridged by Hsglu to form a 1D left-handed staircase-like chain. The staircase-like helix spirals around the pseudo-4₁ screw axis to generate a square-shaped chiral channel with dimensions of 7.645 × 7.529 Å² (Fig. 6). In the helical channel, lattice water molecules are hydrogen bonding to each other in a helical fashion, resulting in a beautiful pattern of “a helical chain inside a helical chain”.

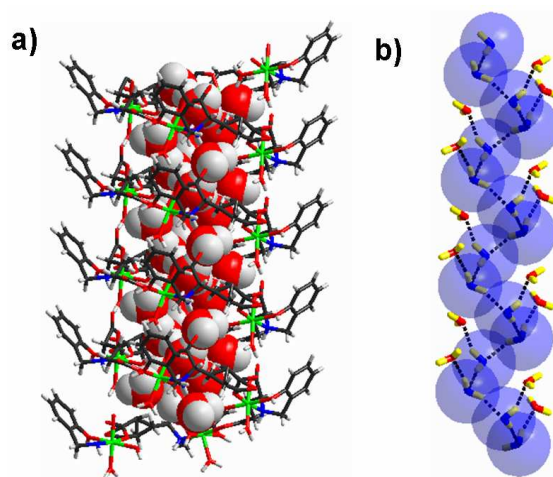


Fig. 6. a) The structure of a helical water chain inside the staircase-like chain in [(H₂O)₂⊂{Ni(Hsglu)(H₂O)₂}]·H₂O; b) A view of the helical water chain interconnected by hydrogen bonding interactions inside the 1D channel. CCDC no. 236742.

Liu and coworkers reported a pair of enantiopure heptanuclear lanthanide clusters, [La₇{(S)-H₂SAsn}₆(CO₃)(NO₃)₆(OCH₃)(CH₃OH)₇].2CH₃OH·5H₂O and [La₇{((R)-H₂SAsn)₆(CO₃)(NO₃)₆(OCH₃)(CH₃OH)₅(H₂O)₂].2CH₃OH·4H₂O, synthesized from Schiff base type ligands (R)-H₂SAsn and (S)-H₂SAsn, derived from salicylaldehyde and L- or D-asparagine.³⁸ In the structures, six ligands connect with

seven lanthanum ions to form an olive-shaped nanocluster in a triple helical pattern (Fig. 7). In the cluster core, a CO_3^{2-} ion derived from atmosphere CO_2 is encapsulated by coordination with three lanthanum ions. Interestingly, the mixture of (S)-SAsn²⁻ and La^{3+} in deionized water has excellent anion-selective recognition ability by picking out CO_3^{2-} from mixed anions of F^- , Cl^- , Br^- , I^- , NO_3^- , SO_4^{2-} , ClO_4^- and CO_3^{2-} .

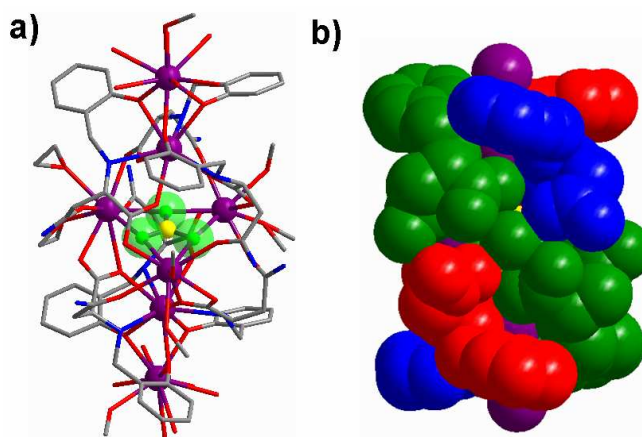


Fig. 7. a) The structure of $[\text{La}_7\{(\text{S})\text{-H}_2\text{SAsn}\}_6(\text{CO}_3)(\text{NO}_3)_6(\text{OCH}_3)(\text{CH}_3\text{OH})_7]$ with a CO_3^{2-} ion inside the core; b) Space-filling representation of the cluster built from triple helices. CCDC no. 701060.

Wu *et al.* have used isonicotinaldehyde to react with amino acids and further reduced to generate a series of pyridine-amino acids for the intention to synthesize higher dimensional homochiral MOCs. Reaction of Py-Ser with Cu^{II} ions afforded a 2D homochiral solid $[\text{Cu}_2(\text{Py-Ser})_2\text{Cl}_2]\cdot\text{H}_2\text{O}$.²⁴ The pyridyl group in Py-Ser plays a key role on the extension of copper-amino carboxylates into a 2D bilayer lamellar framework (Fig. 8). Induced by the chiral carbon center, there are two additional different chiral centers, chiral nitrogen and copper centers, in the structure. Even though $[\text{Cu}_2(\text{Py-Ser})_2\text{Cl}_2]$ contains multiple chiral centers, however, it does not exhibit enantioselectivity in Biginelli reaction of benzaldehyde, urea and ethyl acetoacetate with 90% yield of dihydropyrimidinone. It is interesting that $[\text{Cu}_2(\text{Py-Ser})_2\text{Cl}_2]$ presents high catalytic activity and enantioselectivity in 1,2-addition of Grignard reagent to α,β -unsaturated ketones (aldehyde), in which up to 93% of conversion and

99% of ee value were achieved (Scheme 1). The catalytic property is much superior to that of free ligand, in which the substrate conversion is of 84% with ee value of 51%.

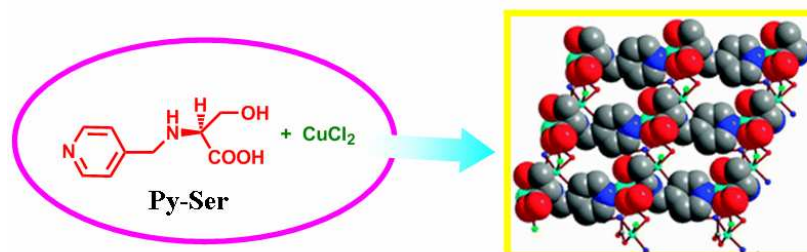
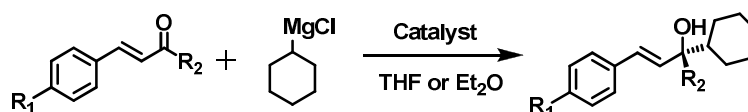


Fig. 8. The synthesis and structure of $[\text{Cu}_2(\text{Py-Ser})_2\text{Cl}_2]$. Reproduced with permission from ref. 24. Copyright 2009 Royal Society of Chemistry. CCDC no. 709104.



Scheme 1. 1,2-addition of α,β -unsaturated ketones catalyzed by $[\text{Cu}_2(\text{Py-Ser})_2\text{Cl}_2]$.

The Wu group further used two amino acid derivatives Py-Asp and Py-Glu to build six homochiral coordination networks, $[\text{Zn}(\text{Py-Asp})(\text{H}_2\text{O})_2]\cdot\text{H}_2\text{O}$, $[\text{Co}(\text{Py-Asp})(\text{H}_2\text{O})_2]\cdot\text{H}_2\text{O}$, $[\text{Zn}(\text{Py-Glu})(\text{H}_2\text{O})_2]$, $[\text{Ni}(\text{Py-Asp})(\text{H}_2\text{O})]\cdot\text{H}_2\text{O}$, $[\text{Cd}_2(\text{Py-Asp})_2(\text{H}_2\text{O})]\cdot 3\text{H}_2\text{O}$ and $[\text{Cd}(\text{Py-Glu})]\cdot\text{H}_2\text{O}$.²⁷ Their framework structures are varied from 1D chains, 2D grid lattices and 3D porous networks, which contain multiple chiral centers of amine groups and metal centers transferred from the chiral carbon centers. Apparently, since different Py-amino acids can be easily synthesized by the similar method, a variety of homochiral MOCPs with diverse framework structures and functionalities will be easily produced.

Sahoo and co-workers reported four homochiral MOCPs based on the enantiomers L- and D-Py-Val, $[\text{Zn}(\text{L-Py-Val})\text{Cl}]\cdot 2\text{H}_2\text{O}$, $[\text{Zn}(\text{L-Py-Val})\text{Br}]\cdot 2\text{H}_2\text{O}$, $[\text{Zn}(\text{D-Py-Val})\text{Cl}]\cdot 2\text{H}_2\text{O}$ and $[\text{Zn}(\text{D-Py-Val})\text{Br}]\cdot 2\text{H}_2\text{O}$, which are structural isomers with different anions (Cl^- or Br^-) or enantiomers with respect to ligand chiralities (D or L).³⁴ In their structures, Py-Val bridges zinc nodes to form a 3D helical *umh*-topology network, containing 1D channels that are filled with water molecules (Fig. 9). Their frameworks remain stable after reversible removal and resorption of

water molecules. Although these MOCPs have similar framework arrangements, they show different properties on water adsorption and proton conductivity. It is interesting that $[\text{Zn}(\text{L-Py-Val})\text{Cl}]$ exhibits higher water affinity, as confirmed by water uptake and release experiments, because the interaction of $\text{O-H}\cdots\text{Cl-Zn}$ is stronger than that of $\text{O-H}\cdots\text{Br-Zn}$. Moreover, due to their different water holding capabilities and electron negativities, the proton conductivities of $[\text{Zn}(\text{L-Py-Val})\text{Cl}]\cdot 2\text{H}_2\text{O}$ and $[\text{Zn}(\text{L-Py-Val})\text{Br}]\cdot 2\text{H}_2\text{O}$ are of $\sim 4.4\times 10^{-5}\text{ Scm}^{-1}$, while $[\text{Zn}(\text{L-Py-Val})\text{Br}]\cdot 2\text{H}_2\text{O}$ and $[\text{Zn}(\text{D-Py-Val})\text{Br}]\cdot 2\text{H}_2\text{O}$ do not have proton conductivity.

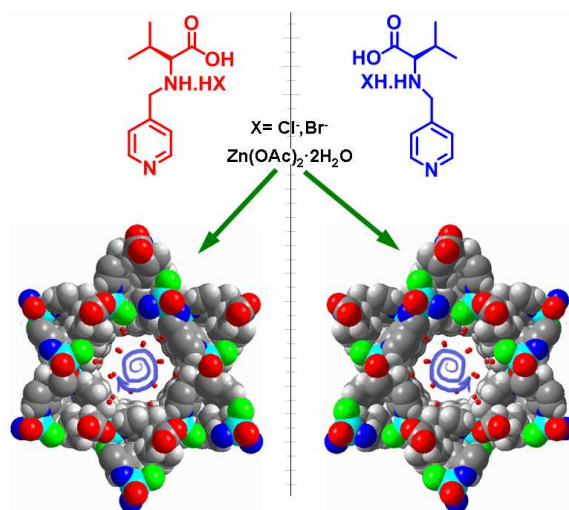


Fig. 9. Space-filling representation of the two enantiomorphs of $[\text{Zn}(\text{L-Py-Val})\text{Cl}]\cdot 2\text{H}_2\text{O}$ and $[\text{Zn}(\text{D-Py-Val})\text{Cl}]\cdot 2\text{H}_2\text{O}$. CCDC nos. 831054 and 831056.

Even though pyridyl group can improve the bridging ability of amino acids, however, it has only one site to coordinate with metal ion per pyridyl group. In order to further improve the bridging abilities of amino acids, Wu and co-workers have used benzoyloxy group instead of pyridyl group to synthesize amino acid derivatives, regarding to the benzoyloxy group has multiple and variable coordination modes. They have used two reduced Schiff bases BA-Val and BA-Ser to construct six homochiral MOCPs $[\text{Zn}(\text{BA-Val})_2(\text{H}_2\text{O})_2]$, $[\text{Cu}_2(\text{BA-Val})_2(\text{H}_2\text{O})_3]$, $[\text{Zn}_2(\text{BA-Val})_2]$, $[\text{Cu}(\text{BA-Ser})(\text{H}_2\text{O})_2]\cdot 2\text{H}_2\text{O}$, $[\text{Zn}(\text{BA-Ser})]$ and $[\text{Cd}_3\text{Na}(\text{BA-Ser})_3(\text{ClO}_4)]\cdot 3\text{H}_2\text{O}\cdot \text{DMF}$.³³ In these MOCPs, the benzoyloxy group

exhibits multiple coordination modes to help formation of the higher dimensional coordination networks. It is interesting that $[\text{Zn}(\text{BA-Ser})]$ and $[\text{Cd}_3\text{Na}(\text{BA-Ser})_3(\text{ClO}_4)]$ have powder SHG intensities of 7.8 and 8.4 versus a-quartz, respectively.

5.2 Homochiral MOCPs built from C-N coupling products

Modification of amino group can also be realized by directed C-N cross coupling reaction of amino group with organic halide under basic conditions. A proline derivative TBPLA (S-1,1',1''-2,46-trimethylbenzene-1,3,4-triyl-tris(methylene)-tris-pyrrolidine-2-carboxylic acid) that has C_3 symmetry was reported by Xiong and co-workers.⁴¹ The solvothermal reaction between TBPLA and Ni^{II} ions afforded a discrete trinuclear Ni^{II} cluster $[\text{Ni}_3(\text{TBPLA})_2(\mu_3\text{-O})(\text{H}_2\text{O})_3]$, which exhibits stable and huge temperature-independent dielectric anisotropic effect (Fig. 10).

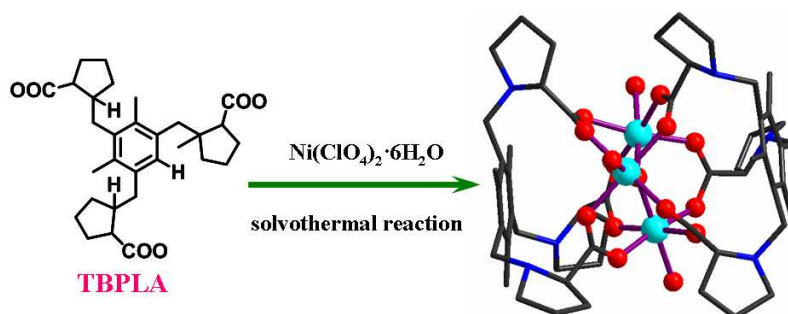


Fig. 10. Schematic diagram for the synthesis of the chiral discrete trinuclear Ni^{II} cluster. CCDC no. 829333.

Wu and co-workers reported two enantiomers of $N,N'N''$ -1,3,5-triazine-2,4,6-triyltris[L(D)-alanine] (L(D)- H_3TTA) by nucleophilic substitution of the amine group with cyanuric chloride.²⁶ Hydrothermal reactions of L- or D- H_3TTA with Cd^{II} ions result two 3D homochiral coordination frameworks $\text{Na}_3[\text{Cd}_2(\text{L-TTA})_2(\mu_2\text{-Cl})](\text{H}_2\text{O})_6$ and $\text{Na}_3[\text{Cd}_2(\text{D-TTA})_2(\mu_2\text{-Cl})](\text{H}_2\text{O})_6$, which have twofold right-handed double helix (P-helix) and twofold left-handed double helix (M-helix), respectively (Fig. 11).

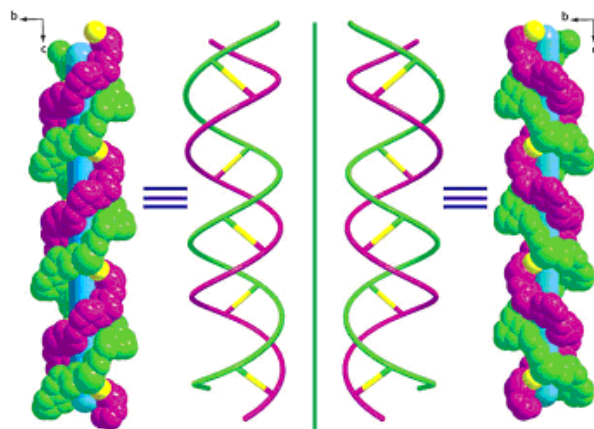
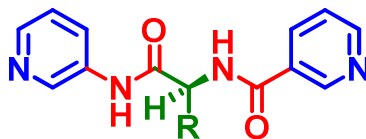


Fig. 11. A view of the double helices in 3D homochiral MOCPs $\text{Na}_3[\text{Cd}_2(\text{L-TTA})_2(\mu_2\text{-Cl})](\text{H}_2\text{O})_6$ (left) and $\text{Na}_3[\text{Cd}_2(\text{D-TTA})_2(\mu_2\text{-Cl})](\text{H}_2\text{O})_6$ (right). Reproduced with permission from ref. 26. Copyright 2010 Royal Society of Chemistry. CCDC nos. 784200 and 784201.

5.3 Homochiral MOCPs built from amide-type ligands



Scheme 2. Bis-pyridyl-bis-amide ligands derived from L-phenylalanine, L-alanine and L-leucine. BisPy-Ala, R = Me; BisPy-Phe, R = CH_2Ph ; BisPy-Leu, R = tBu .

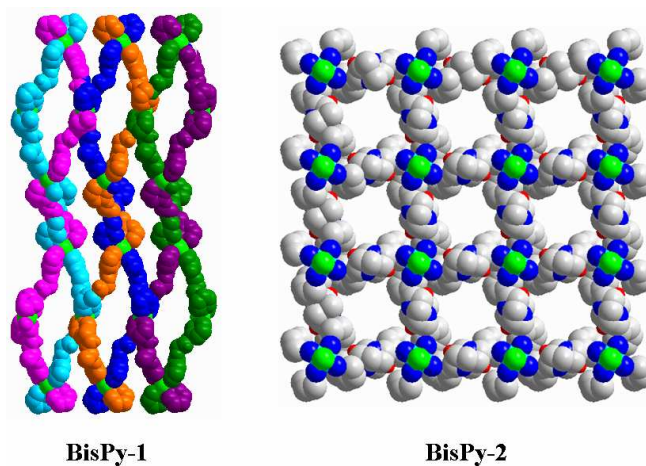


Fig. 12. Views of the structures of BisPy-1 and BisPy-2. CCDC nos. 699625 and 699626.

Both carboxylic acid and amino groups of amino acids can also be modified in the same ligands just like in the synthesis of peptides. Dastidar and co-workers have synthesized three bis-pyridyl-bis-amide type ligands derived from L-phenylalanine, L-alanine and L-leucine (Scheme 2).⁴² Since this type of ligands is neutral, the structures of homochiral MOCPs can be further tuned by different anions to modify their properties. The two 3D homochiral MOCPs $\{\text{Cu}(\mu\text{-BisPy-Phe})_2\text{Cl}_2\} \cdot 2\text{H}_2\text{O}$ (BisPy-1) and $\{\text{Cu}(\mu\text{-BisPy-Ala})_2\text{Cl}_2\} \cdot x\text{H}_2\text{O}$ (BisPy-2) are constructed from the bis-pyridyl-bis-amide ligands and chloride anions. BisPy-1 is made up of intertwined P-helical coordination polymeric chains with a pitch of ~ 40 Å, while BisPy-2 is a 3D porous framework containing noninterpenetrated octahedral chiral micropores (Fig. 12). The desolvated sample BisPy-2 displays sponge-like behavior that can be dissolved in water and recrystallized upon evaporation of solvent.

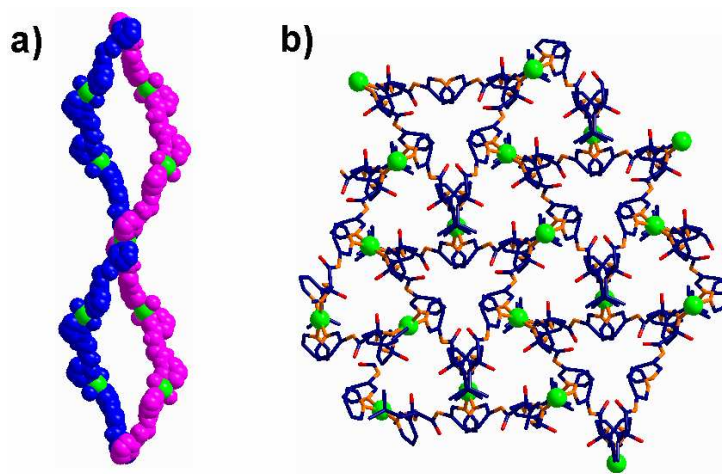
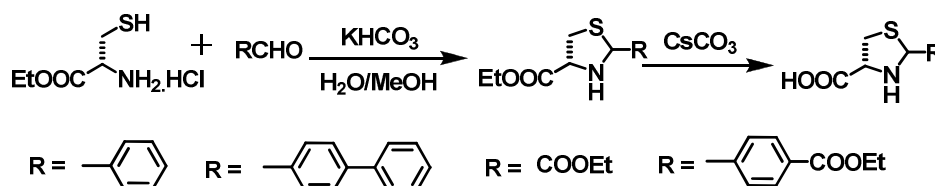


Fig. 13. Illustration of the crystal structure of $\{\text{Cu}(\mu\text{-BisPy-Leu})_2\text{Cl}_2\} \cdot 2\text{H}_2\text{O}$, (a) a part of the intertwined helices and (b) the 3D coordination network. CCDC no. 838097.

Since the bi-pyridine type ligands are neutral, different anions should have very important roles on the formation of different coordination networks. However, the four isomorphous homochiral MOCPs $\{\text{Cu}(\mu\text{-BisPy-Phe})_2\text{Br}_2\} \cdot 2\text{H}_2\text{O}$, $\{\text{Cu}(\mu\text{-BisPy-Ala})_2(\text{H}_2\text{O})\text{Br}\} \cdot \text{Br} \cdot 4\text{H}_2\text{O}$, $\{\text{Cu}(\mu\text{-BisPy-Leu})_2\text{Br}_2\} \cdot 2\text{H}_2\text{O}$ and $\{\text{Cu}(\mu\text{-BisPy-Leu})_2\text{Cl}_2\} \cdot 2\text{H}_2\text{O}$ can be safely isolated even in the presence of

additional different anions, such as NO_3^- , SO_4^{2-} , ClO_4^- and BF_4^- .⁴³ Their structures are 3D helical intertwined microporous coordination networks, which crystallize in the cubic space group $P3_22_1$ (Fig. 13). The Br analogues have interesting properties to separate Cu^{II} ions from a mixed ions of Cu^{II} , Co^{II} and Zn^{II} with efficiency of >98%, and Br^- ions from a mixture of Br^- , NO_3^- , SO_4^{2-} , ClO_4^- and BF_4^- by in situ crystallization. These results well demonstrate the hard-soft-acid-base principle and Irving-William series for separation of Cu^{II} ions and the Hofmeister bias for separation of Br^- ions. Inspired by these interesting results, the authors further studied the role of SiF_6^- among different oxoanions (SO_4^{2-} , ClO_4^- , NO_3^- and OTf^-) during the self-assembling process.⁴⁴ SiF_6^- prevents the formation of a quartz-like MOCP, while the other anions such as ClO_4^- and NO_3^- generate the quartz-like MOCPs, and OTf^- and SO_4^{2-} result in the 3D non-interpenetrated octahedral channels.

5.4 Homochiral MOCPs built from cyclized amino acids



Scheme 3. Cyclization of L-cysteine with aldehydes.

There are a few amino acids bearing special R groups with specific chemical reactivity, which make us have different pathways to modify natural amino acids. Rossin and coworkers reported the cyclized products of amino acids by condensation of -SH and -NH₂ groups of L-cysteine with aldehydes under basic conditions with retained chirality (Scheme 3).³⁰ Hydrothermal reaction of $\text{CoCl}_2 \cdot 6\text{H}_2\text{O}$ and thiazolidine-2,4-dicarboxylated acid (H_2TDA) results a 3D homochiral MOCP $[\text{Co}(\text{TDA})(\text{H}_2\text{O})] \cdot \text{H}_2\text{O}$. In the crystal structure, as shown in Fig. 14, there are two kinds of micro-channels, one hydrophobic (with the exposed sulfur atoms) and one hydrophilic (with the exposed water ligands), which can take up CO_2 molecules at 273 K with the maximum of 4.7 wt% at 920 torr.

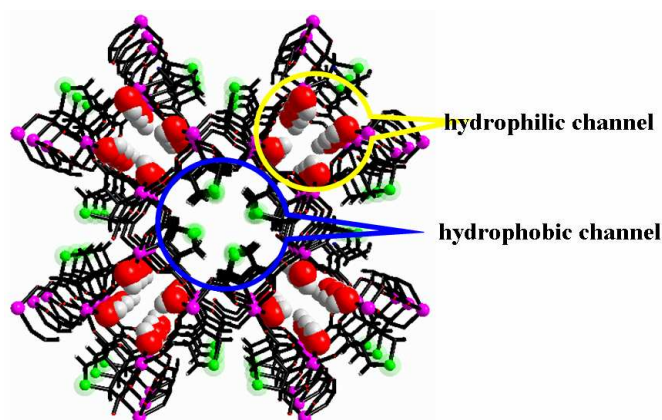


Fig. 14. A view of the 3D framework of $[\text{Co}(\text{TDA})(\text{H}_2\text{O})]$ with two kinds of micro-channels. CCDC no. 855629.

5.5 Homochiral MOCPs containing dangling amino acids

Using amino acids as a part of the backbones of organic ligands is the most simple and straightforward pathway for the transformation of chirality from amino acids to coordination networks. However, there are some difficulties in controlling the functionalities and porosities of homochiral MOCPs. Alternatively, dangling amino acid residues onto highly porous MOCPs is much more convenient in realization of their different chirality-related applications.

Telfer *et al.* reported a porous homochiral MOCP by employing a N-Boc-proline decorated ligand as building block (Fig. 15).²⁵ Because the Boc group can not only prevent the proline residue to coordinate with zinc ions but also avoid framework interpenetration, the N-Boc-proline appended biphenyl-4,4'-dicarboxylate ligand is therefore connected with Zn^{II} ions to form a non-interpenetrated structure IRMOF-Boc-Pro with cubic topology. Dangling N-Boc-proline on organic ligand successfully results in the incorporation of amino acid residues onto the framework of IRMOF. Moreover, the catalytic functionality can be simply realized by thermal treatment of IRMOF-Boc-Pro to remove Boc group for the formation of IRMOF-Pro via single-crystal to single-crystal (SCSC) pathway, while IRMOF-Pro cannot be directly prepared by using Boc-protected ligand under the similar synthesis conditions. With proline units in the pores of ~ 5 to 10.5 \AA in diameters, IRMOF-Pro efficiently catalyzes the asymmetric aldol reaction of acetone with

4-nitrobenzaldehyde, in which 4-hydroxy-4-(4-nitrophenyl)pentan-2-one was produced with 29% of ee value. IRMOF-Boc-Pro is inactive to the aldol reaction under otherwise identical conditions, indicating that the unprotected pyrrolidine groups are responsible for the catalytic activity. The superiority of this N-Boc-proline dangling strategy is to preclude framework interpenetration and ensure large vacant space around the catalytic sites by following deprotection.

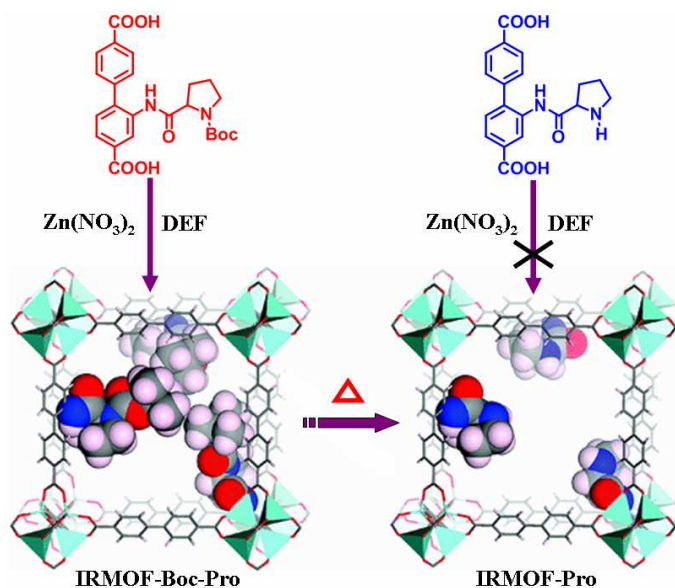
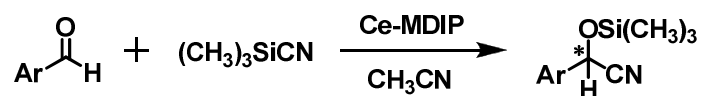


Fig. 15. Synthesis of IRMOF-Boc-Pro from N-Boc-proline decorated ligand and generation of IRMOF-Pro *via* SCSC pathway. Reproduced with permission from ref. 25. Copyright 2011 American Chemical Society. CCDC nos. 818115 and 818116.

By using L- and D-pyrroline-2-yl-imidazole (PYI) as chiral adducts, two enantiomorphs Ce-MDIP1 and Ce-MDIP2 were prepared by the Duan group, which have 1D channels and unsaturated metal coordination sites.²⁰ As demonstrated above, since the pyrroline group will cause great problems for crystallization, they have used N-protected L- and D-N-tert-butoxy-carboxyl-2-(imidazole)-1-pyrrolidine (L- and D-BCIP) as chiral adducts under solvothermal reaction conditions to synthesize Ce-MDIP1 and Ce-MDIP2, respectively. Due to the weak coordination affinity between N atoms and lanthanide ions, the chiral adducts L- and D-BCIP are not incorporated into the frameworks. In the structure of Ce-MDIP1, the 3D coordination

network contains 1D chiral channels with dimensions of $10.5 \times 6.0 \text{ \AA}^2$ (Fig. 16). Ce-MDIP1 exhibits excellent activity on cyanosilylation of aldehydes with $(\text{CH}_3)_3\text{SiCN}$, in which up to 98% of ee value has been achieved (Scheme 4). Similarly, Ce-MDIP2 also catalyzes the cyanosilylation with high efficiency to result the enantiomers. Since the chiral adducts are not incorporated into Ce-MDIP1 and Ce-MDIP2, the chirality of the catalytic products should be controlled by the whole chiral environments around substrate molecules.



Scheme 4. Cyanosilylation of aldehydes catalyzed by Ce-MDIPs.

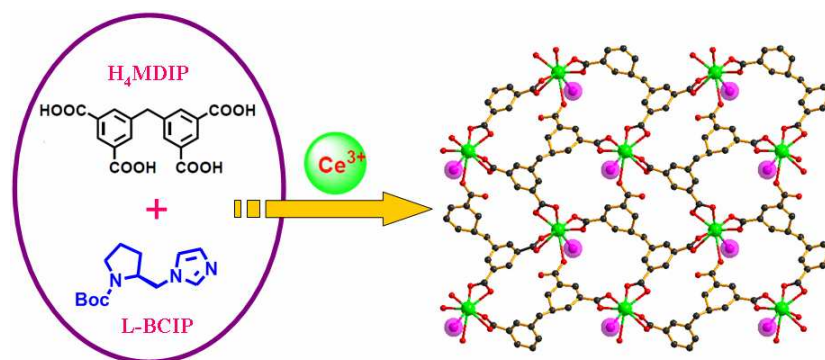


Fig. 16. Schematic representation of the synthesis and the 3D network of Ce-MDIP1 containing chiral channels. CCDC no. 822520.

Afterwards, they used the chiral adduct L-BCIP, 1,3,5-tris(4-carboxyphenyl)benzene (H_3BTB) and cadmium perchlorate to synthesize a porous homochiral MOCP Cd-BTB. As shown in Fig. 17, Cd-BTB adopts a 2D honeycomb network with rhombus channels of $4.0 \times 6.5 \text{ \AA}^2$ in dimensions. Interestingly, the Boc protecting group on the pyrrolidine moiety was spontaneously removed during the formation of L-PYI. The L-PYI moiety, terminally coordinating with the cadmium ions, is located above and below the 2D layer. Cd-BTB exhibits moderate catalytic activity on aldol reaction, in which 61% of ee value has been achieved in the reaction between 3-nitrophenyl and cyclohexanone (Scheme 5).

Because the pore size of the framework is too small to accommodate substrate molecules, the reaction thus takes place on solid surfaces of the homochiral MOCP.

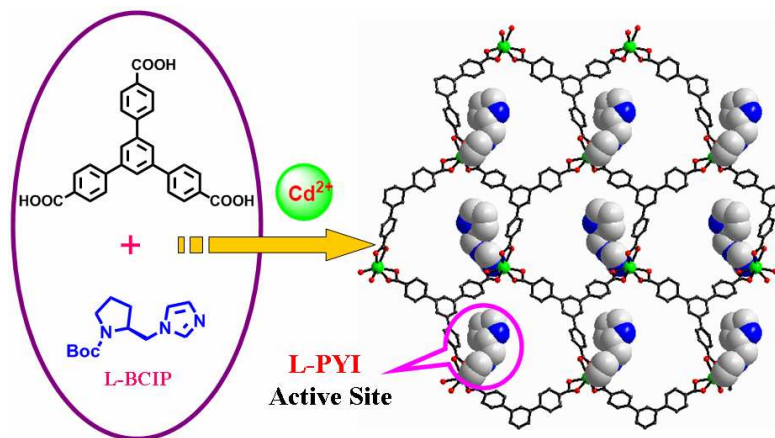
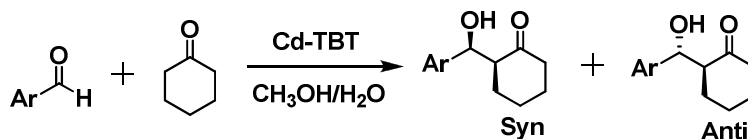


Fig. 17. Schematic representation of the synthesis and the 2D honeycomb network of Cd-BTB with active sites in the pores. CCDC no. 822522.



Scheme 5. Aldol reaction of aldehydes with cyclohexanone.

The Duan group further reported a photoactive chiral MOCP Zn-BCIP1 synthesized from solvothermal reaction of 4,4',4''-tricarboxyltriphenylamine (H₃TCA) and Zn(NO₃)₂·6H₂O in the presence of L-BCIP.²¹ The structure of L-BCIP is a 2D brick wall layer structure that is built from 3-connected binuclear zinc nodes and 4,4',4''-nitrilotribenzoate bridges. The L-BCIP moieties are located inside the 1D channels of 12 × 16 Å² in dimensions by coordinating with zinc ions. Deprotection of the proline unit is accomplished by simply heating, which results a new compound Zn-PYI1 with retained crystallinity and chirality (Fig. 18). Since triphenylamine moiety can initiate photoinduced single electron transfer from its excited state to acceptor during photo reaction, Zn-PYI1 is efficient on photocatalytic alkylation of aldehydes coupled with diethyl 2-bromomalonate. High reaction efficiency (74% of

yield) and excellent enantioselectivity (92% of ee) were achieved in the reaction of phenylpropyl aldehyde with 2-bromomalonate (Scheme 6). Similarly, the enantiomorph Zn-PYI2 also exhibits high catalytic efficiency to produce the product of opposite chirality. To make comparison, they further synthesized a lanthanide compound Ho-TCA which is a 3D porous coordination framework that has the similar topology with MOF-150.⁴⁶ Ho-TCA catalyzes the reaction of phenylprophaldehyde with diethyl 2-bromomalonate to afford the α -alkylation product with yield of 86% and ee value of 20% in the presence of 20% L-PYI as organocatalyst. The different catalytic activities between Zn-PIY1 and the mixture of Ho-TCA and L-PYI suggest that integration of photocatalyst and asymmetric organocatalyst into a single framework has the superior enantioselectivity by restriction of the movement of substrate molecules in the chiral channels.

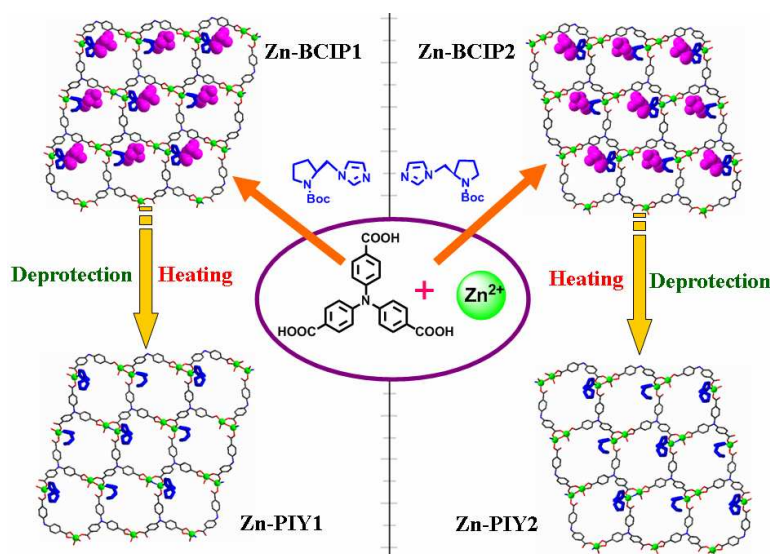
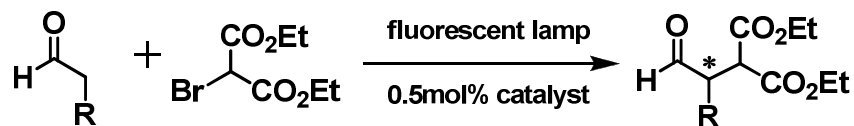


Fig. 18. Illustration of the mirror image structures of Zn-BCIP1 and Zn-BCIP2 and their deprotected forms Zn-PIY1 and Zn-PIY2. CCDC no. 943903.



Scheme 6. The photocatalytic α -alkylation reaction of aliphatic aldehydes.

6. Post-modification of MOCPs with amino acid derivatives

To date, most of the homochiral MOCPs are based on chiral ligands by transfer chirality from chiral moieties to the whole coordination networks. However, special synthesis strategies are often required to grow high quality crystals for single crystal X-ray diffraction analysis because chiral ligands bear specific orientation and low symmetries which may bring some difficulties in crystallizing MOCPs, whereas harsh synthesis conditions (high temperature, basic intermedium) often give rise to partial or even full racemization.⁴⁷ Recently, post-modification was developed as an emerging strategy for the preparation of homochiral MOCPs by attaching chiral moieties onto achiral rigid porous coordination frameworks under suitable conditions. A significant advantage of this approach is to convert chemically and thermally robust coordination networks into homochiral materials by attaching suitable chiral moieties.

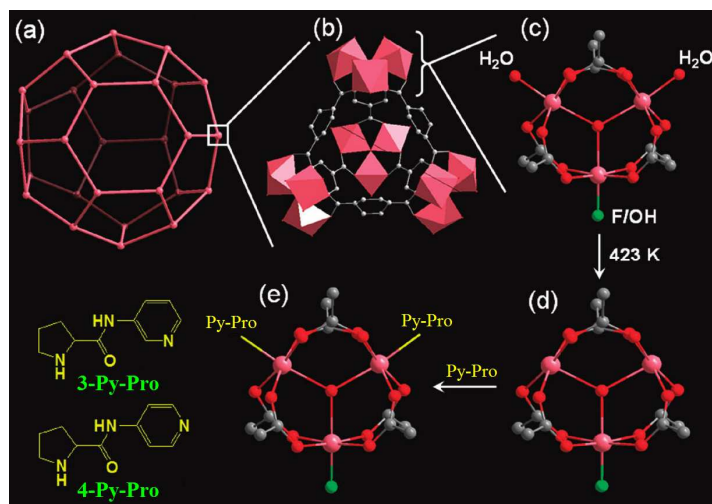
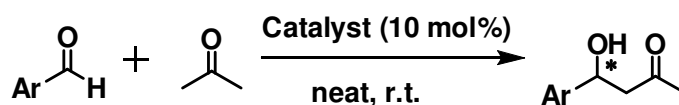


Fig. 19. Deconstruction diagram of CMILs by post-modification of MIL-101 with chiral moieties. Reproduced from ref. 22 with permission from the American Chemical Society. CCDC no. 605510.

Kim and coworkers reported the first example of catalytically active homochiral MOCPs prepared from achiral MIL-101 by post-modification.^{22,48} They attached L-proline derivatives [(S)-N-(pyridin-3-yl)-pyrrolidine-2-carboxamide] (3-Py-Pro) and [(S)-N-(pyridin-4-yl)-pyrrolidine-2-carboxamide] (4-Py-Pro) onto the open metal

sites in MIL-101, and thus realize their highly efficient asymmetric catalysis. Post-modification of MIL-101 was achieved by treating with chiral ligands 3-Py-Pro and 4-Py-Pro, which result two new porous homochiral MOCPs $[\text{Cr}_3\text{O}(\text{3-Py-Pro})_{1.8}(\text{H}_2\text{O})_{0.2}\text{F}(\text{bdc})_3] \cdot 0.15(\text{H}_2\text{bdc}) \cdot \text{H}_2\text{O}$ (CMIL-1) and $[\text{Cr}_3\text{O}(\text{4-Py-Pro})_{1.75}(\text{H}_2\text{O})_{0.25}\text{F}(\text{bdc})_3] \cdot 0.15(\text{H}_2\text{bdc}) \cdot \text{H}_2\text{O}$ (CMIL-2), respectively (Fig. 19). The incorporated CMILs are highly efficient on asymmetric aldol reaction of aromatic aldehydes with ketones, in which up to 90% of yield and 80% of ee value were achieved (Scheme 7). It is interesting that the two heterogeneous catalysts exhibit much higher enantioselectivity than their homogeneous chiral counterparts, because the movement of substrate molecules is restricted by the chiral pores of CMILs. The excellent results indicate that the post-modification strategy is a convenient pathway for the generation of higher porous chiral MOCPs for highly efficient heterogeneous asymmetric catalysis.



Scheme 7. Aldol reaction of aldehydes with acetone.

7. Conclusions

Natural amino acids are a class of chiral and functional molecules, which have been used as active sites in many functional materials. Considering that most of the natural amino acids only contain one carboxylate group and one amino group per amino acid which often prevent the formation of higher porous homochiral MOCPs, several effective strategies have been therefore developed for the intention to improve the porosity of homochiral MOCPs. Since amino acids prone to chelate metal ions, introduction of the secondary rigid bridging ligands, such as 4,4'-bpy, can substantially improve the opportunity for the construction of porous homochiral MOCPs. Oligo-peptides synthesized from condensation of amino acids are also efficient chiral ligands for the synthesis of porous homochiral MOCPs. Moreover, the amino groups on amino acids are easily to react with different moieties which can

supply multiple amino acid derivatives, such as to react with aldehyde for the formation of Schiff bases, to react with phenyl halogen for the formation of C-N cross-coupling products, to react with acyl chlorides for the formation of amides, and to cyclize the amino acids between amino and special R groups. Introduction of additional coordination sites onto amino acids have greatly improved the porosity of homochiral MOCPs. Furthermore, dangling amino acid residues on the pore surfaces of rigid porous MOCPs by in situ synthesis or post-modification is also an effective strategy. The amino acid residues incorporated homochiral MOCPs present many interesting properties that are derived from amino acid residues and the porous nature of MOCPs. They have been realized applications in various fields of asymmetric catalysis, luminescence, adsorption, separation, magnetics, second-order nonlinear optics and conduction. Being a class of biologically active units, the homochiral MOCPs that consist of amino acid synthons will definitely receive more and more attention and should be on an explosive growth in the near future.

Acknowledgements

We thank the NSF of China (Grant No. 21073158 and 21373180), Zhejiang Provincial Natural Science Foundation of China (Grant No. Z4100038), the Fundamental Research Funds for the Central Universities (Grant No. 2013FZA3006), and the research fund of Key Laboratory for Advanced Technology in Environmental Protection of Jiangsu Province (AE201312) for financial support.

References

- 1 (a) J. R. Long and O. M. Yaghi Ed., Themed issues on metal-organic frameworks, *Chem. Soc. Rev.*, 2009, **38**, 1213; (b) H.-C. Zhou, J. R. Long and O. M. Yaghi Ed., Metal-Organic Frameworks special issue, *Chem. Rev.*, 2012, **112**, 673.
- 2 (a) L. J. Murray, M. Dincă and J. R. Long, *Chem. Soc. Rev.*, 2009, **38**, 1294; (b) S. S. Han, J. L. Mendoza-Cortés and W. A. Goddard III, *Chem. Soc. Rev.*, 2009, **38**, 1460; (c) J. R. Li, J. Sculley and H.-C. Zhou, *Chem. Rev.*, 2012, **112**, 869.
- 3 (a) L. Ma, C. Abney and W. Lin, *Chem. Soc. Rev.*, 2009, **38**, 1248; (b) J. Lee, O. K.

- Farha, J. Roberts, K. A. Scheidt, S. T. Nguyen and J. T. Hupp, *Chem. Soc. Rev.*, 2009, **38**, 1450; (c) A. Corma, H. García and F. X. Llabrés i Xamena, *Chem. Rev.*, 2010, **110**, 4606.
- 4 (a) M. D. Allendorf, C. A. Bauer, R. K. Bhaktaa and R. J. T. Houka, *Chem. Soc. Rev.*, 2009, **38**, 1330; (b) Y. Cui, Y. Yue, G. Qian and B. Chen, *Chem. Rev.*, 2012, **112**, 1126.
- 5 (a) L. E. Kreno, K. Leong, O. K. Farha, M. Allendorf, R. P. Van Duyne and J. T. Hupp, *Chem. Rev.*, 2012, **112**, 1105. (b) M. D. Allendorf, C. A. Bauer, R. K. Bhakta and R. J. T. Houk, *Chem. Soc. Rev.*, 2009, **38**, 1330.
- 6 M. Kurmoo, *Chem. Soc. Rev.*, 2009, **38**, 1353
- 7 C. Wang, T. Zhang and W. Lin, *Chem. Rev.*, 2012, **112**, 1084.
- 8 (a) D. Zacher, O. Shekhah, C. Wöll and R. A. Fischer, *Chem. Soc. Rev.*, 2009, **38**, 1418; (b) A. Bétard and R. A. Fischer, *Chem. Rev.*, 2012, **112**, 1055.
- 9 (a) P. Horcajada, C. Serre, M. Vallet-Regí, M. Sebban, F. Taulelle and G. Férey, *Angew. Chem. Int. Ed.*, 2006, **45**, 5974; (b) J. D. Rocca, D. Liu and W. Lin, *Acc. Chem. Res.*, 2011, **44**, 957.
- 10 (a) C.-D. Wu, A. Hu, L. Zhang and W. Lin, *J. Am. Chem. Soc.*, 2005, **127**, 8940; (b) M. Yoon, R. Srirambalaji and K. Kim, *Chem. Rev.*, 2012, **112**, 1196.
- 11 (a) G. Li, W. Yu and Y. Cui, *J. Am. Chem. Soc.*, 2008, **130**, 4582; (b) T. Liu, Y. Liu, W. Xuan and Y. Cui, *Angew. Chem., Int. Ed.*, 2010, **122**, 4215.
- 12 Z. Guo, R. Cao, X. Wang, H. Li, W. Yuan, G. Wang, H. Wu and J. Li, *J. Am. Chem. Soc.*, 2009, **131**, 6894.
- 13 (a) C.-D. Wu and W. Lin, *Angew. Chem., Int. Ed.*, 2007, **46**, 1075; (b) L. Ma and W. Lin, *Angew. Chem., Int. Ed.*, 2009, **48**, 3637; (c) L. Ma, D. J. Mihalcik and W. Lin, *J. Am. Chem. Soc.*, 2009, **131**, 4610.
- 14 (a) G. Li, W. Yu, J. Ni, T. Liu, Y. Liu, E. Sheng and Y. Cui, *Angew. Chem., Int. Ed.*, 2008, **47**, 1245; (b) G. Li, W. Yu and Y. Cui, *J. Am. Chem. Soc.*, 2008, **130**, 4582.
- 15 B. Sreenivasulu and J. J. Vittal, *Angew. Chem., Int. Ed.*, 2004, **43**, 5769.
- 16 H.-Y. An, E.-B. Wang, D.-R. Xiao, Y.-G. Li, Z.-M. Su and L. Xu, *Angew. Chem., Int. Ed.*, 2006, **45**, 904.

- 17 J. Rabone, Y.-F. Yue, S. Y. Chong, K. C. Stylianou, J. Bacsá, D. Bradshaw, G. R. Darling, N. G. Berry, Y. Z. Khimyak, A. Y. Ganin, P. Wiper, J. B. Claridge and M. J. Rosseinsky, *Science*, 2010, **329**, 1053.
- 18 A. D. Naik, M. M. Dîrtu, A. P. Railliet, J. Marchand-Brynaert and Y. Garcia, *Polymers*, 2011, **3**, 1750.
- 19 D. Bradshaw, J. B. Claridge, E. J. Cussen, T. J. Prior and M. J. Rosseinsky, *Acc. Chem. Res.*, 2005, **38**, 273.
- 20 D. Dang, P. Wu, C. He, Z. Xie and C. Duan, *J. Am. Chem. Soc.*, 2010, **132**, 14321.
- 21 P. Wu, C. He, J. Wang, X. Peng, X. Li, Y. An and C. Duan, *J. Am. Chem. Soc.*, 2012, **134**, 14991.
- 22 M. Banerjee, S. Das, M. Yoon, H. J. Choi, M. H. Hyun, S. M. Park, G. Seo and K. Kim, *J. Am. Chem. Soc.*, 2009, **131**, 7524.
- 23 J. Canivet, S. Aguado, G. Bergeret and D. Farrusseng, *Chem. Commun.*, 2011, **47**, 11650.
- 24 M. Wang, M.-H. Xie, C.-D. Wu and Y.-G. Wang, *Chem. Commun.*, 2009, 2396.
- 25 D. J. Lun, G. I. N. Waterhouse and S. G. Telfer, *J. Am. Chem. Soc.*, 2011, **133**, 5806.
- 26 Q. Zhu, T. Sheng, R. Fu, C. Tan, S. Hua and X. Wu, *Chem. Commun.*, 2010, **46**, 9001.
- 27 X.-L. Yang, M.-H. Xie, C. Zou, F.-F. Sun and C.-D. Wu, *CrystEngComm*, 2011, **13**, 1570.
- 28 L. Dong, W. Chu, Q. Zhu and R. Huang, *Cryst. Growth Des.*, 2011, **11**, 93.
- 29 E. V. Anokhina, Y. B. Go, Y. Lee, T. Vogt and A. J. Jacobson, *J. Am. Chem. Soc.*, 2006, **128**, 9957.
- 30 A. Rossin, B. D. Credico, G. Giambastiani, M. Peruzzini, G. Pescitelli, G. Reginato, E. Borfecchia, D. Gianolio, C. Lambertic and S. Bordiga, *J. Mater. Chem.*, 2012, **22**, 10335.
- 31 R. Vaidhyanathan, D. Bradshaw, J.-N. Rebilly, J. P. Barrio, J. A. Gould, N. G. Berry and M. J. Rosseinsky, *Angew. Chem., Int. Ed.*, 2006, **45**, 6495.
- 32 (a) L.-F. Ma, L.-Y. Wang, X.-K. Huo, Y.-Y. Wang, Y.-T. Fan, J.-G. Wang and S.-H.

- Chen, *Cryst. Growth Des.*, 2008, **8**, 620; (b) A. C. Kathalikkattil, K. K. Bisht, N. Aliaga-Alcalde and E. Suresh, *Cryst. Growth Des.*, 2011, **11**, 1631.
- 33 X.-L. Yang, M.-H. Xie, C. Zou and C.-D. Wu, *CrystEngComm*, 2011, **13**, 6422.
- 34 S. C. Sahoo, T. Kundu and R. Banerjee, *J. Am. Chem. Soc.*, 2011, **133**, 17950.
- 35 E. V. Anokhina and A. J. Jacobson, *J. Am. Chem. Soc.*, 2004, **126**, 3044.
- 36 A. Manton, L. Massüger, P. Rabu, C. Palivan, L. B. McCusker and A. Taubert, *J. Am. Chem. Soc.*, 2008, **130**, 2517.
- 37 C. Martí-Gastaldo, J. E. Warren, K. C. Stylianou, N. L. O. Flack and M. J. Rosseinsky, *Angew. Chem., Int. Ed.*, 2012, **51**, 11044.
- 38 X.-L. Tang, W.-H. Wang, W. Dou, J. Jiang, W.-S. Liu, W.-W. Qin, G.-L. Zhang, H.-R. Zhang, K.-B. Yu and L.-M. Zheng, *Angew. Chem., Int. Ed.*, 2009, **48**, 3499.
- 39 (a) Y. Xie, Z. Yu, X. Huang, Z. Wang, L. Niu, M. Teng and J. Li, *Chem. Eur. J.*, 2007, **13**, 9399; (b) J.-N. Rebilly, J. Bacsá and M. J. Rosseinsky, *Chem. Asian J.*, 2009, **4**, 892; (c) Z.-Z. Li, L. Du, J. Zhou, M.-R. Zhu, F.-H. Qian, J. Liu, P. Chen and Q.-H. Zhao, *Dalton Trans.*, 2012, **41**, 14397; (d) J. He, G. Zhang, D. Xiao, H. Chen, S. Yan, X. Wang, J. Yang and E. Wang, *CrystEngComm*, 2012, **14**, 3609; (e) T. Kundu, S. C. Sahoo and R. Banerjee, *Cryst. Growth Des.*, 2012, **12**, 4633; (f) C.-T. Yang, M. Vetrichelvan, X. Yang, B. Moubaraki, K. S. Murray and J. J. Vittal, *Dalton Trans.*, 2004, 113.
- 40 R. Ganguly, B. Sreenivasulu and J. J. Vittal, *Coord. Chem. Rev.*, 2008, **252**, 1027.
- 41 D.-W. Fu, Y.-M. Song, G.-X. Wang, Q. Ye, R.-G. Xiong, T. Akutagawa, T. Nakamura, P. W. H. Chan and S. D. Huang, *J. Am. Chem. Soc.*, 2007, **129**, 5346.
- 42 S. Banerjee, N. N. Adarsh and P. Dastidar, *CrystEngComm*, 2009, **11**, 746.
- 43 S. Banerjee and P. Dastidar, *Cryst. Growth Des.*, 2011, **11**, 5592.
- 44 S. Banerjee, N. N. Adrash and P. Dastidar, *CrystEngComm*, 2013, **15**, 245.
- 45 (a) H. Y. Lee, J. Park, M. S. Lah and J.-I. Hong, *Cryst. Growth Des.*, 2008, **8**, 587; (b) D. L. Reger, A. P. Leitner and M. D. Smith, *Inorg. Chem.*, 2012, **51**, 10071; (c) L.-F. Ma, L.-Y. Wang, X.-K. Huo, Y.-Y. Wang, Y.-T. Fan, J.-G. Wang and S.-H. Chen, *Cryst. Growth Des.*, 2008, **8**, 620.
- 46 H. K. Chae, J. Kim, O. D. Friedrichs, M. O'Keefe, O. M. Yaghi, *Angew. Chem., Int.*

Ed., 2003, **42**, 3907.

47 C.-D. Wu, L. Li, L.-X. Shi, *Dalton Trans.*, 2009, **34**, 6790.

48 G. Férey, C. Mellot-Draznieks, C. Serre, F. Millange, J. Dutour, S. Surblé and I. Margiolaki, *Science*, 2005, **309**, 2040.

Graphical Abstract:

The recently developed strategies on the designed synthesis of porous homochiral MOCPs based on amino acid residues and their interesting properties are summarized in this Highlight.

